Electronic Supplementary Material (ESI) for Journal of Materials Chemistry A.
This journal is © The Royal Society of Chemistry 2021

Electronic Supplementary Information for

Nanoscale Pt_5Ni_{36} Design and Synthesis for Efficient Oxygen Reduction Reaction in Proton Exchange Membrane Fuel Cell

Xiaolu Liu,[a] Xin Wan,[c] Xiaoli Tan,[a] Hui Yang,*[a] Yu Yang,*[b] Jianglan Shui,*[c] and Xiangke Wang[a]

Emails: h.yang@ncepu.edu.cn; yang_yu@iapcm.ac.cn; shuijianglan@buaa.edu.cn

[a]*College of Environmental Science and Engineering, North China Electric Power University, Beijing, 102206, P. R. China.*

[b]*LCP, Institute of Applied Physics and Computational Mathematics Beijing 100088, P. R. China.*

[c]*School of Materials Science and Engineering, Beihang University, Beijing 100191, P. R. China.*

Experimental Section

Chemicals $H_2PtCl_6 \cdot 6H_2O$, $NiCl_2 \cdot 6H_2O$, dimethylformamide (DMF), and ethylalcohol were purchased from Aladdin. Polyacrylonitrile (PAN) and perchloric acid were purchased from Sigma-Aldrich. All chemicals used in the synthesis of self-designed catalysts are analytical regents (AR) and used without further purification.

Characterizations The scanning electron microscope (SEM) images were obtained by HITACHI S-4800. TEM images were received by using a JEOL-2010 microscope with an accelerating voltage of 200 kV. X-ray diffraction (XRD) were obtained by Scintag-XDS-2000 diffractometer with Cu Kα radiation (λ= 1.5418 Å). X-ray photoelectron spectroscopy (XPS) measurements via a VG Scientific ESCALAB Mark II spectrometer, equipping with a monochromatic Al Kα radiation and low-energy electron-flooding for charge compensation. The electron storage ring energy was 2.5 GeV and the maximum storage beam current was 250 mA. The energy of the X-ray was detuned using a fixed-exit double-crystal Si (111) monochromator. Ionization chambers with N_2 atmosphere were used to collect the Ni K-edge spectra in transmission mode at room temperature. The EXAFS data were analyzed using standard procedures with the program IFEFFIT.

Electrochemical Measurements All electrochemical tests were performed on the CHI 760E electrochemical workstation with a three-electrode electrochemical cell. The saturated calomel electrode (SCE) was regarded as a reference electrode, platinum counter electrode, and 0.1 M $HClO_4$ aqueous solution as electrolytes. The catalyst ink was prepared by ultrasonically 5 mg of catalyst powder dispersed into 1 mL of

ethanol (including 10 μL 5 wt% Nafion). The continuous oxygen flow was kept over the electrolyte during the test to guarantee O_2 saturation. A rotating ring-disk electrode was served as the substrate for the working electrode. RRDE tests were detected by using the American Pine Instruments device.

Rotating ring-disk electrode (RRDE) measurements of the samples were carried out to test the ring current (I_{ring}) at a disk rotation rate of 1600 rpm. The peroxide yield (H_2O_2%) and the electron transfer number (n) were calculated by the following equations:

$$\mathrm{n} = 4 \times \frac{I_{disk}}{\left(\frac{I_{ring}}{N}\right) + I_{disk}}$$

$$H_2O_2(\%) = 200 \times \frac{I_{ring}}{\left(\frac{I_{ring}}{N}\right) + I_{disk}}$$

Where I_{disk} and I_{ring} are the disk and ring currents, respectively. *N* is the ring current collection efficiency that is 0.42.

PEMFC tests The 12 mg (mass fraction of Pt was 7.2 wt%) Pt_5Ni_{36}/CNFs catalyst and Pt/C were mixed with Nafion® alcohol solution, isopropanol and deionized water to prepare the catalyst ink. Then deal ink with subjected to a sonication and stirring. The will dispersed ink was dropped on 5 cm^{-2} of carbon paper (cathode Pt load was 0.129 mg_{Pt} cm^{-2} for Pt_5Ni_{36}/CNFs and 0.1 mg_{Pt} cm^{-2} for Pt/C, and the anode was 0.2mg_{Pt} cm^{-2}), drying in vacuum at 80 °C for 2 h. The prepared cathode and anode were pressed on both sides of Nafion 211 film (DuPont) for 90 seconds at a pressure of 1.5 MPa and a temperature of 130 °C to obtain a membrane electrode assembly (MEA). Polarization plots were recorded using fuel cell test station (Scribner 850e).

UHP-grade H_2 and O_2 humidified at 80 °C were supplied to the anode and cathode at a flow rate of 0.3 and 0.4 L min^{-1}, respectively. The cell temperature was maintained at 80 °C and the backpressures at both electrodes were set at1.0 bar. Then a 30 h stability test was performed on the same MEA, while the flow rates of the gas was switched to 0.1 L min^{-1} for both electrodes.

Density Functional Theory Calculations The density functional theory (DFT) calculations were carried out by using the Vienna *ab initio* simulation package (VASP)[1]. The Perdew–Burke–Ernzerhof (PBE)[2] form of generalized gradient approximation (GGA) and the projector-augmented wave potential[3] were employed to describe the exchange–correlation energy and the electron–ion interaction, respectively. The cutoff energy for the plane-wave expansion was set to 400 eV. A Fermi broadening of 0.05 eV was chosen in all *ab initio* calculations to smear the occupation of the bands around the Fermi energy, by a finite-*T* Fermi function[4]. We adopted optPBE exchange functional for the van der Waals correlation to describe the dispersion forces within the adsorption system[5-7]. optPBE is an optimized PBE-style functional, yielding a low mean absolute deviation from the CCSD(T) results on the S22 set (a set of 22 weakly interacting dimers) and precise descriptions for molecular hexamers[6, 7]. The platinum $5d^96s^1$, nickel $3d^84s^2$, carbon $2s^22p^2$, oxygen $2s^22p^4$, and hydrogen $1s^1$ electrons were treated as valence electrons. The optimized lattice constants of Pt and Ni were 3.98 Å and 3.43 Å respectively.

The Ni (111), Pt (111), and alloyed surfaces in this work were all modeled by six atomic monolayers with a periodic (3 × 3) surface supercell, and a vacuum spacing of

20 Å along surface normal direction (z). We randomly built 8 alloyed surfaces with one or three Ni atoms in the topmost surface layer. Atoms of the two bottom atomic layers were fixed during structural relaxations. The horizontal lattices of the alloyed surfaces were fully relaxed. The Brillouin zone integrations were calculated using 5 × 5 × 1 Monkhorst−Pack[8] *k*-point meshes.

The adsorption of CO molecules were simulated on the relaxed surfaces within the NVT ensemble with the time step of 1 femtosecond, by using first-principles molecular dynamics (FPMD) method. The adsorption energy was defined as the energy required to adsorb, i. e., $E_{ad} = E_{(slab+mol)} - E_{slab} - E_{mol}$, where $E_{(slab+mol)}$, E_{slab}, and E_{mol} represent for the free energies of the adsorbed slabs, of the slabs and of the CO molecules. We run different FPMD trajectories for CO adsorbing at different surface areas (stretched Ni or compressed Ni). After reaching thermodynamic equilibrium through 3 picoseconds of FPMD simulations, the adsorption energies of CO molecules were collected over 200 time steps. The phonon energies of different surfaces were neglected in our study.

Supplementary Figures

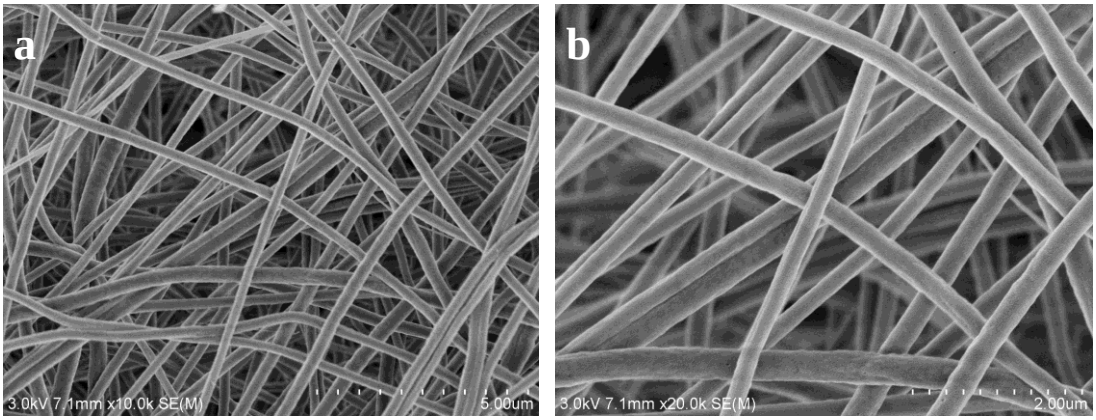

Fig. S1. (a, b) SEM images of polyacrylonitrile fiber after stabilized at 533 K.

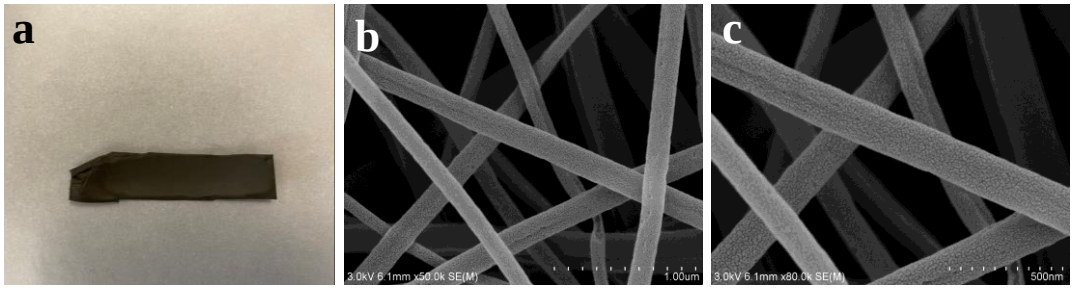

Fig. S2. (a) Photograph and (b, c) SEM images of carbon nanofibers.

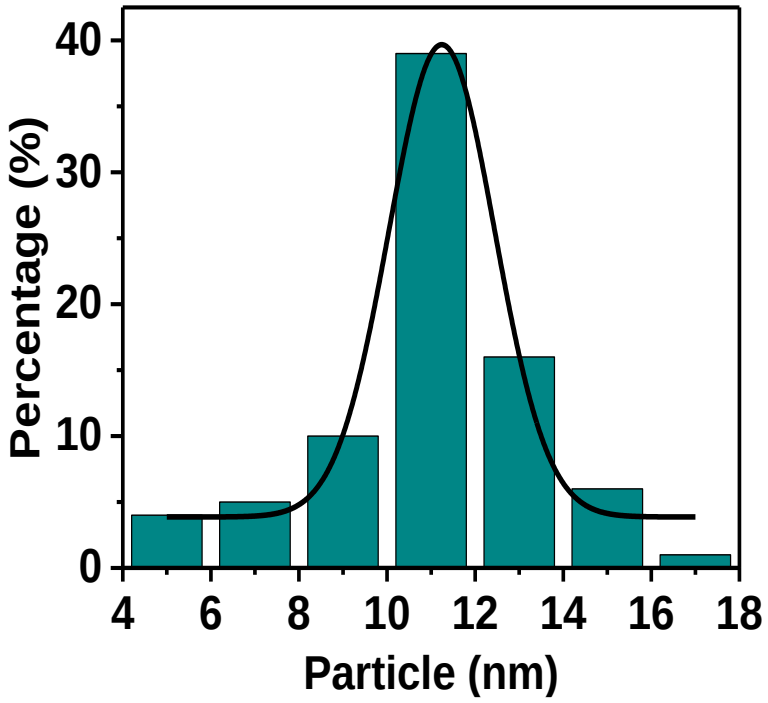

Fig. S3 Histogram of nanoparticle sizes in Pt_5Ni_{36}/CNFs.

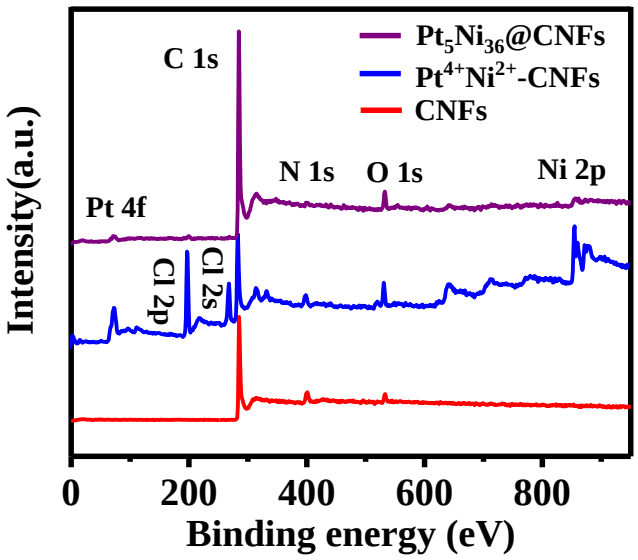

Fig. S4. XPS spectra of Pt_5Ni_{36}/CNFs, $Pt^{4+}Ni^{2+}$/CNFs and CNFs.

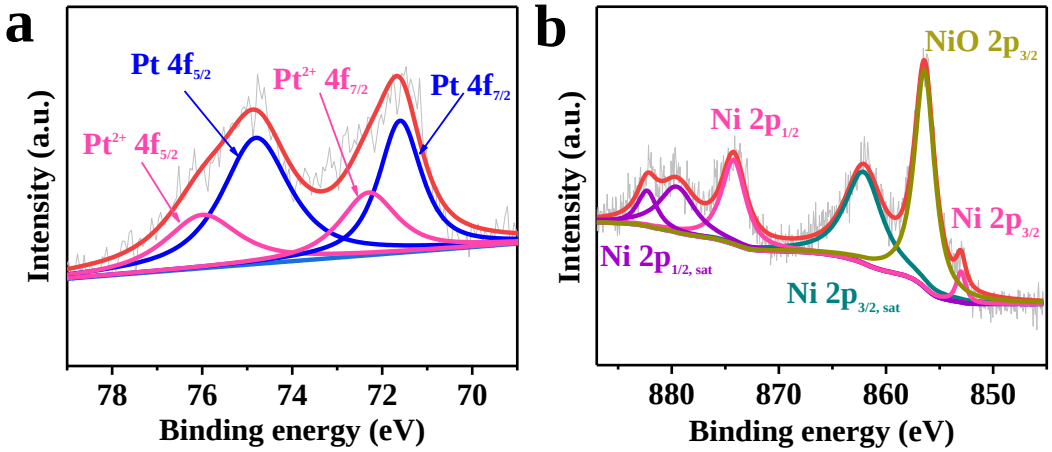

Fig. S5 High-resolution XPS spectra of (a) Pt 4f, and (b) Ni 2p in the Pt_5Ni_{36}/CNFs.

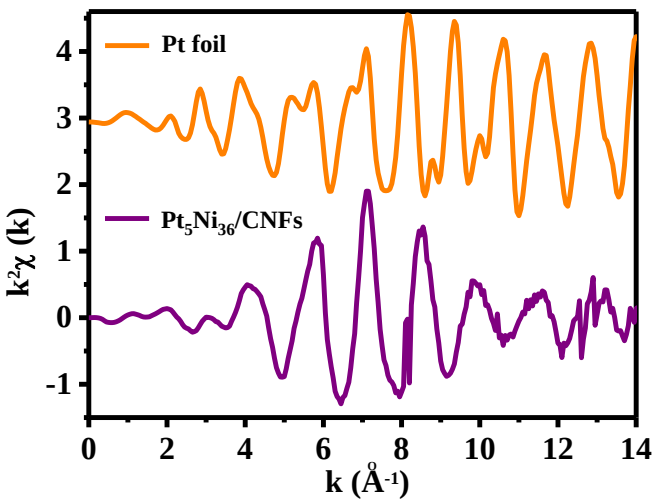

Fig. S6. Corresponding radial structure functions of Pt in Pt foil and Pt_5Ni_{36}/CNFs.

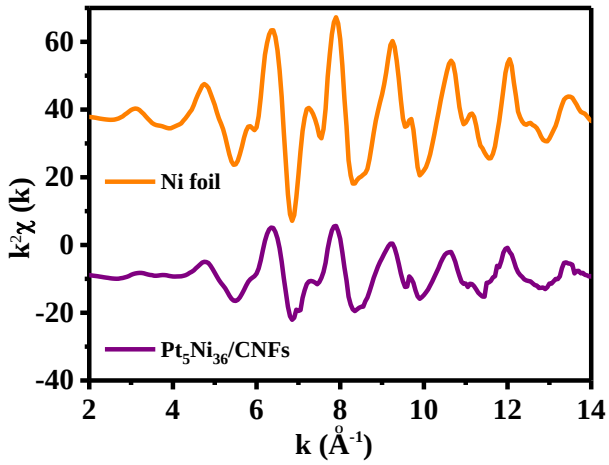

Fig. S7. Corresponding radial structure functions of Ni in Ni foil and Pt_5Ni_{36}/CNFs.

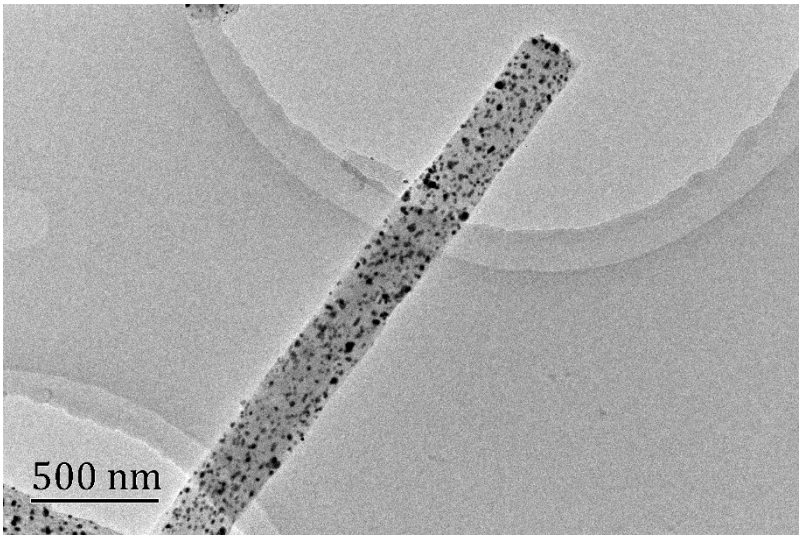

Fig. S8. TEM image of Pt_5Ni_{36}/CNFs after stability test.

Supplementary Tables

Table S1 Mass fraction of Pt and Ni in Pt_5Ni_{36}/CNFs analyzed by ICP-MS.

Element	Wt% (icp)
Ni	14.47
Pt	6.7

Table S2 Fitting results of Pt L3-edge for the metal cores and the metal-metal distances of Pt foil and PtNi alloy nanoparticle (bond lengths in Å).

Sample	Shell	R(Å)	N	σ2	R-factor
Pt foil	Pt-Pt	2.77	10.1	0.0046	0.0016
Pt_5Ni_{36}/C	Pt-Ni	2.56	6.7	0.0075	0.0101
	Pt-Pt	2.69	0.9	0.0024	

Table S3 Fitting results of Ni K edge for the metal cores and the metal-metal distances of Ni foil and PtNi alloy nanoparticle (bond lengths in Å).

Sample	Shell	R(Å)	N	σ2	R-factor
Ni foil	Ni-Ni	2.48	9.6	0.0060	0.0009
Pt_5Ni_{36}/C	Ni-O	2.04	1.3	0.0004	0.0086
	Ni-Ni	2.50	4.8	0.0057	
	Ni-Pt	2.56	6.7	0.0081	

Table S4 Acidic H_2-O_2 Fuel cell performance and Pt consumption in whole cell at peak power density and 80 ºC

Samples	Pt consumption/g_{Pt} kW^{-1}	Backpressure	References
Pt_5Ni_{36}/CNFs	**0.118 g_{Pt} kW^{-1}**	**1.0bar**	**This work**
$Pt_{1.1}/BP_{defect}$	0.134 g_{Pt} kW^{-1}	0.5bar	Ref.9
Pt_1-N/BP	0.13 g_{Pt} kW^{-1}	0.2 bar	Ref.10
Pt-NfnPPy	0.34 g_{Pt} kW^{-1}	1.5 bar	Ref.11
Pt/VC–PANI	0.95 g_{Pt} kW^{-1}	~1.0 bar	Ref.12
PtNi@Pt/C	0.167 g_{Pt} kW^{-1}	0.8 bar	Ref.13
Sputter 180	0.22 g_{Pt} kW^{-1}	~2.0 bar	Ref.14
Sputter (0.1 mg_{Pt} cm^{-2})	1.56 g_{Pt} kW^{-1}	~1.5 bar	Ref.15

References

1. G. Kresse, J. Furthmüller, *Phys. Rev. B,* 1996, **54**, 11169-11186.
2. J. P. Perdew, K. Burke, M. Ernzerhof, *Phys. Rev. Lett.,* 1996, **77**, 3865-3868.
3. P. E. Blöchl, *Phys. Rev. B,* 1994, **50**, 17953-17979.
4. G. Román-Pérez, J. M. Soler, *Phys. Rev. Lett.,* 2009, **103**, 096102.
5. M. Dion, H. Rydberg, E. Schröder, D. C. Langreth, B. I. Lundqvist, *Phys. Rev. Lett.,* 2004, **92**, 246401.
6. J. Klimeš, D. R. Bowler, A. Michaelides, *Condens. Matter,* 2010, **22**, 022201.
7. J. Klimeš, D. R. Bowler, A. Michaelides, *Phys. Rev. B,* 2011, **83**, 195131.
8. H. J. Monkhorst, J. D. Pack, *Phys. Rev. B,* 1976, **13**, 5188-5192.
9. J. Liu, M. Jiao, B. Mei, Y. Tong, Y. Li, M. Ruan, W. Xu, *Angew. Chem. Int. Ed*., 2019, **58**, 1163-1167.
10. J. Liu, M. Jiao, L. Lu, H. M. Barkholtz, Y. Li, Y. Wang, L. Jiang, Z. Wu, D. j. Liu, L. Zhuang, C. Ma, J. Zeng, B. Zhang, D. Su, P. Song, W. Xing, W. Xu, Y. Wang, Z. Jiang, G. Sun, *Nat. Common*., 2017, **8**, 15938.
11. Z. Xia, S. Wang, L. Jiang, H. Sun, S. Liu, X. Fu, B. Zhang, D. Su, J. Wang, G. Sun, *Sci. Rep*., 2015, **5**, 1-11.
12. K. Kakaei, *Fuel Cells,* 2012, **12**, 939-945
13. J. Choi, J. H. Jangb, C. W. Roha, S. Yangc, J. Kima, J. Lima, S. J. Yoob, H. Lee, *Appl. Catal*. *B Environ*., 2018, **225**, 530-537
14. M. S. Çögenli, S. Mukerjee, A. B. Yurtcan, *Fuel Cells*, 2015, **15**, 288-297
15. Y. C. Lai, K. L. Huang, C. H. Tsai, W. J. Lee, Y. L. Chen, *Int. J. Energy Res*., 2012, **36**, 918-927.